

Estimation of Fracture Toughness of Reactor Pressure Vessel Steels Using Automated Ball Indentation Test

Thak Sang Byun, Joo Hark Kim, Bong Sang Lee, Ji Hyun Yoon, and Jun Hwa Hong
Korea Atomic Energy Research Institute
P.O.Box 105 Yusong, Taejon, 305-600, Korea

Abstract

The automated ball indentation (ABI) test was utilized to develop a semi-nondestructive method for estimating the fracture toughness (K_{JC}) in the transition temperature range. The key concept of the method is that the indentation deformation energy to the load at which the mean ball-specimen contact pressure reaches the fracture stress is related to the fracture energy of the material. ABI tests were performed for the reactor pressure vessel (RPV) base and weld metals at the temperatures of $-150^{\circ}\text{C} \sim 0^{\circ}\text{C}$ and the fracture toughness (estimated K_{JC}) was calculated from the indentation load-depth data. For all steels the temperature dependence of the estimated fracture toughness was almost the same as that of the ASTM K_{JC} master curve. The reference temperatures (T_o) of the steels were determined from the estimated K_{JC} versus temperature curves. The reference temperature was well correlated with the index temperature of 41J Charpy impact energy (T_{41J}).

1. Introduction

In the assessment of structural material integrity the automated ball indentation (ABI) test is an attractive test technique since it is in nature semi-nondestructive and requires a relatively small material volume. Further the ABI technique makes it possible to perform portable/*in situ* test on in-service components such as reactor pressure vessel and power plant pipe lines.

Many theories and models have been developed to measure the mechanical properties of materials with ball indentation techniques [1-5] and some fundamental mechanical properties, especially tensile parameters such as yield and ultimate strengths and stress-strain curve, now can be measured by the current ABI test technology [6-8]. However, because the indentation does not induce cracking, the estimation of fracture toughness from indentation data has been rarely studied for ductile metals [6].

This work is an attempt to develop a methodology for estimating the fracture toughness of ferrite steels from the ABI test data. In the following sections a new theory is described, based on the concept that the indentation deformation energy to the load at which the mean ball-specimen contact pressure reaches the fracture stress is related to the fracture energy of the material. Also the concept of temperature-independent cleavage fracture stress [9,10] and Meyer law [1,4,5] are used as bases. This paper also includes the application results for nine RPV steels including five base metals and four weld metals. The main conclusion is that the fracture toughness master curves (K_{JC} versus temperature) can be obtained from the indentation load-depth data through the proposed theory.

2. Theory of Indentation Deformation Energy to Fracture

2.1. Indentation Deformation Energy to Fracture

To correlate the indentation deformation energy with fracture toughness, the following bases are considered:

(1) The indentation on material surface produces a deformed region beneath the indenter, which is dependent on the shape of indenter and the magnitude of applied load. The indentation with a small indenter causes highly concentrated deformation field near the indenter-material contact. The crack(or notch) also give rise to stress concentration. It is thought that there is an analogy between the deformation fields beneath a small indenter and ahead of a crack. Also, the degree of stress concentration may depend on the diameter of the spherical indenter and the root radius of the crack, respectively. If the fracture toughness is interpreted as the deformation capability of material under the concentrated stress fields, it is possible to correlate the fracture energy with the indentation deformation energy.

(2) In the indentation deformation the stress in the loading direction is compressive, while that causing crack growth in the fracture toughness test specimens is tensile. However it is generally accepted that, if not cyclic (in case of cyclic loading the Baushinger effect reduces the strength on reversed deformation), the compressive and tensile deformations are equivalent.

(3) On ductile metals the indentation with usual ball indenter can not generate any crack. This indicates that an additional criterion which corresponds to final fracture should be introduced to the indentation deformation in order to correlate with the fracture energy. The additional criterion to be imposed to the indentation deformation of ductile metals is the cleavage fracture stress. It has been known that the cleavage fracture stress in ferritic steels is nearly independent of test temperature[9,10]. The following method for the estimation of fracture toughness from indentation load-depth data is developed based on the concept of constant fracture stress. Thus the application may be limited to the transition and lower temperature range.

It is postulated that the indentation deformation energy(per unit contact area) to the load at which the mean contact pressure reaches the fracture stress is related to the fracture energy of the material. The indentation deformation energy per unit contact area, W_{ID} , is defined as

$$W_{ID} = \frac{4}{\pi d_f^2} \int_0^{h_f} P dh \quad (2-1)$$

where P is applied load, h indentation depth, and h_f and d_f are the depth and the chordal diameter of indentation impression when the mean contact pressure is equal to the fracture stress. Usually the RPV steels reveal almost linear indentation load-depth curve; $P = Sh$, where S is the slope of the linear curve. Then, with $h_f = P_f / S$, W_{ID} is expressed by

$$W_{ID} = \frac{2}{\pi S} \left(\frac{P_f}{d_f} \right)^2 \quad (2-2)$$

Introducing the criterion for fracture that the mean contact pressure, P_m^f , is equal to fracture stress, σ_f :

$$P_m^f = \frac{4P_f}{\pi d_f^2} = \sigma_f \quad (2-3)$$

and using the Meyer law[1,4,5]:

$$\frac{P_f}{d_f^2} = A\left(\frac{d_f}{D}\right)^{m-2} \quad (2-4)$$

where A is material yield parameter, m Meyer index, and D is spherical ball diameter, then the final form of the indentation deformation energy to fracture becomes

$$W_{ID} = \frac{2A^2 D^2}{\pi S} \left(\frac{\pi \sigma_f}{4A}\right)^{\frac{2m-2}{m-2}} \quad (2-5)$$

On the other hand, the toughness parameters, such as Charpy impact energy and static fracture toughness(K_{JC}), versus temperature have non-zero lower shelves even at very low temperatures. Thus the fracture energy per unit area, W_f , can be given by

$$W_f = W_0 + W_T \quad (2-6)$$

where W_0 is the lower shelf energy(per unit area), the fracture surface formation energy and pure elastic energy may exert this term, and W_T is the temperature-dependent energy. The later term might be related to the plastic deformation and become main portion of total fracture energy at the transition temperatures. In this study we regarded the indentation deformation energy to fracture as the temperature-dependent energy; $W_T = W_{ID}$.

2.2. Fracture Stress

To obtain the value of W_{ID} with equation (2-5), the evaluation of fracture stress is an important procedure in addition to the ABI tests to obtain the values of A , S , and m . The fracture stress can be obtained through the notched bar specimen tests[11,12] or calculated from fracture toughness and yield stress[10]. In the present work, however, we attempted to calculate the fracture stress from fracture toughness, K_{JC} , data and ABI data. Since the fracture stress is nearly independent of test temperature, if at least one low temperature fracture toughness is available, it can be obtained by coupling the indentation deformation energy with fracture theories.

For a crack of length $2a$ in infinite plate, the fracture toughness is given by

$$K_{JC} = \sigma_F \sqrt{\pi a} \quad (2-7)$$

where σ_F is the uniformly-applied stress when the fracture occurs, and according to the generalized Griffith theory[13], σ_F is

$$\sigma_F = \sqrt{\frac{2EW_f}{\pi a}} \quad (2-8)$$

Then the relationship between fracture energy and fracture toughness becomes

$$W_f = \frac{K_{JC}^2}{2E} \quad (2-9)$$

For the ferritic steels the fracture toughness (median value) versus temperature curve in the transition temperature range is expressed by the master curve[14]:

$$K_{JC} (med) = 30 + 70e^{0.019(T-T_0)}, \quad MPa\sqrt{m} \quad (2-10)$$

where T_0 is the reference temperature. In this curve the lower shelf of fracture toughness is $30 MPa\sqrt{m}$. Accordingly with equation (2-9) the lower shelf energy, W_0 , is calculated to be $2143 J/m^2$. With the equations (2-5), (2-6), and (2-9) the fracture stress is calculated from fracture toughness available, ABI data, and W_0 as follows:

$$\sigma_f = \frac{4A}{\pi} \left[\frac{\pi S(W_f - W_0)}{2A^2 D^2} \right]^{\frac{m-2}{2m-2}} \quad (2-11)$$

3. Experimental

3.1 Materials and Specimens

The test materials comprise five SA508 Cl.3 RPV base metals and four RPV weld metals. Table 1 contains the chemical compositions of the steels. The base metals are in quenched and tempered and post-weld heat treated state and the weld metal in post-weld heat treated state. The Charpy-sized rectangular bars (10mm × 10 mm × 55 mm) cut from the 1/4 thickness locations of RPVs were used in ABI tests.

3.2 ABI Test

An automated ball indentation test system of ATC (model: PortaFlow-P1) was used for indentation tests. The indenter used was WC ball of 0.508 mm diameter. A specially designed bath was installed on the ABI test system for low temperature tests, on which the test temperature was controlled by liquid nitrogen in an accuracy of $\pm 2^\circ\text{C}$. Fig. 1 is the schematic of indenter head and bath. The indentation tests were performed at the temperatures of $-150^\circ\text{C} \sim 0^\circ\text{C}$ with an indentation speed of 0.0076 mm/sec (0.0003 inch/sec), which gives an average strain rate of about 10^{-2} sec^{-1} for the deformed region.

4. Results and Discussion

4.1 Fracture Stress

The fracture stress was calculated by equation (2-11) and illustrated in Fig. 2. The fracture stresses of base metals are in the range of 2200 MPa ~ 2600 MPa and those of weld metals in the range of 2400 ~ 2800 MPa. These values are close to those of the steels with similar microstructures; 2130 MPa ~ 2250 MPa for A533B steels[9,10], 2270 MPa ~ 2450 MPa for C-Mn base and weld metals and Ti-B weld metals[11], and 2100 MPa ~ 2900 MPa for quenched and tempered steels[12]. Fig. 2 includes 2 ~ 4 fracture toughness data for each test material. The averages of those 2 ~ 4 data were used in the fracture toughness calculation.

4.2 Fracture Toughness Transition Curve

The fracture toughness, K_{JC} , was calculated with the equations (2-5), (2-6), and (2-9) and the transition temperature curves (master curves) were obtained by regression of the estimated

K_{JC} data for $-150^{\circ}\text{C} \sim 0^{\circ}\text{C}$. Table 2 contains the fitted master curves. According to the master curve method[14], the transition of fracture toughness with temperature can be described by one parameter; the reference temperature, T_0 , since the other coefficients of the curve are the same for whole ferritic steels, as indicated in equation (2-10). Then all master curves of different ferritic steels will overlap on one curve if the independent variable is given by the temperature relative to T_0 ; $T - T_0$.

The q values evaluated with the present method are in the range of 0.0166 to 0.0218 and the average is 0.0194, which is very close to that of the ASTM K_{JC} master curve; 0.019. This parameter determines the shape of fracture toughness transition curve and the reference temperature, T_0 , determines the position of the curve.

The estimated K_{JC} values are illustrated in Figs. 3 and 4 with the ASTM master curve($K_{JC}(\text{median})$ vs. $T - T_0$) and two bounding curves(dotted) of 5% and 95% fracture probabilities. Most estimated K_{JC} data are within the two dotted curves. In conclusion the postulations described in the section 2 are considered to be reasonable.

4.3 Comparison of Fracture Toughnesses and Transition Temperatures

In Fig. 5 the estimated K_{JC} data are compared with the K_{JC} data which obtained from 1T-CT or 1/2T-CT specimens. The fracture toughnesses less than $200 \text{ MPa}\sqrt{\text{m}}$ are compared to exclude the data of upper shelf. Although Fig. 5 shows large data scattering, there is a good linear proportionality between the estimated K_{JC} and the measured K_{JC} .

On the other hand, Fig. 6 shows the comparison of T_0 and T_{41J} (the index temperature when Charpy impact energy is 41 J). The two transition temperatures are linearly proportional to each other. The fitted curve reveals a cut-off value of -31.1°C , which seems to be originated from the difference of strain rate between the testings; ABI or K_{JC} tests are static tests and Charpy impact test is a dynamic test.

5. Conclusions

A semi-nondestructive method for estimating the fracture toughness(K_{JC}) in the transition temperature range was developed on the bases of the theories and models for continuous ball indentation and cleavage fracture. The method developed was applied to the evaluation of the fracture toughnesses of RPV steels at the temperatures of $-150^{\circ}\text{C} \sim 0^{\circ}\text{C}$. The application results are summarized as follows:

[1] For all steels tested the temperature dependence of estimated K_{JC} was almost the same as that of the ASTM K_{JC} master curve; the temperature dependence of estimated K_{JC} was well described by the function of the form $e^{q(T-T_0)}$, where all q values were within the range of $0.0166 \sim 0.0218$ and the average was 0.0194.

[2] The reference temperatures, T_0 , of the steels were determined from the estimated K_{JC} versus temperature curves. The reference temperature was well correlated with the index temperature of Charpy impact energy, T_{41J} .

[3] In this work the fracture stresses were obtained from low temperature K_{JC} data available. It is necessary to develop a simpler method to obtain the fracture stress for more effective applications.

Acknowledgment

This work is a part of the Structural Steels(Reactor Materials) Development Program financed by the Ministry of Science and Technology .

6. References

- [1] E. Meyer, Z. Ver. Dtsch Ing., 52 (1908) p645, 740, and 835.
- [2] R.A. George, S. Dinda, and A. S. Kasper, Metal Progress (1976) p30-35.
- [3] H.A. Francis, J. of Eng. Mater. and Tech.(Tr. ASME), Vol. 98, No.3 (1976) p272-281.
- [4] D. Tabor, Proc. Roy. Soc. 192A (1948) p247-274.
- [5] D. Tabor, J. of Inst. of Metals, 79 (1951) p1-18.
- [6] F.M. Haggag, ASTM STP 1204 (1993) p27-44.
- [7] T.S. Byun, J.H. Kim, S.H. Chi, and J.H. Hong, Proc. of the 10th Conf. on Mech. Behaviors of Materials, Ansan, Korea, Oct. (1996) p 497-505.
- [8] T.S. Byun, J.H. Kim, S.H. Chi, and J.H. Hong, Proc. of the 6th Symp. on Mater. Degradation and Lofe Prediction, Seoul, Korea, Nov. (1996) p 167-176.
- [9] J.F. Knott, Micromechanisms of Plasticity and Fracture, p261-302.
- [10] J. Markin and A.S. Telelman, Engi. Fracture Mech., Vol. 3, (1971) p151-167.
- [11] J.H. Chen, H. Ma, and G.Z. Wang, Metal. Trans. 21A (1990) p313-320.
- [12] Z. Xiulim, Engi. Fracture Mech., Vol. 33, No. 5 (1989) p685-695.
- [13] T.L. Anderson, Fracture Mechanics, CRC press, (1995) p41.
- [14] ASTM standard Draft 13: Test Method for the Determination of Reference Temperature, T_0 , for Ferritic Steels in the Transition Range (Rev. 7-1-1997).

Table 1. Chemical compositions of SA508 Cl.3 RPV steels and weld metals

Material	Chemical Composition										Remarks
	C	Mn	Si	Al	Ni	Cr	Mo	P	S	Cu	
HB1	0.17	1.39	0.08	0.004	0.77	0.04	0.49	0.007	0.003	0.05	Base Metal
HB2	0.20	1.42	0.07	0.005	0.79	0.15	0.57	0.007	0.003	0.06	Base Metal
HB3	0.17	1.41	0.06	0.006	0.84	0.15	0.51	0.006	0.002	0.03	Base Metal
HB4	0.19	1.35	0.09	0.009	0.82	0.16	0.52	0.008	0.004	0.04	Base Metal
HB5	0.21	1.36	0.24	0.022	0.92	0.21	0.49	0.007	0.002	0.03	Base Metal
HW1	0.07	1.73	0.22	0.009	0.07	0.05	0.52	0.015	0.004	0.02	Weld Metal
HW2	0.07	1.69	0.26	0.01	0.11	0.06	0.53	0.016	0.004	0.02	Weld Metal
HW3	0.08	1.72	0.29	0.01	0.18	0.06	0.50	0.009	0.002	0.03	Weld Metal
HW4	0.08	1.74	0.26	0.01	0.13	0.05	0.51	0.011	0.002	0.03	Weld Metal

Table 2. Parameters of fracture toughness master curves

Fracture Toughness Master Curve: $K_{JC}(T) = 30 + 70e^{q(T-T_0)}$ MPa \sqrt{m}		
Material	q	T ₀
HB1	0.0206	-32.4
HB2	0.0196	-40.0
HB3	0.0218	-37.1
HB4	0.0215	-64.5
HB5	0.0181	-88.6
HW1	0.0193	-74.9
HW2	0.0166	-53.2
HW3	0.0189	-45.2
HW4	0.0186	-57.8
Average = 0.0194		

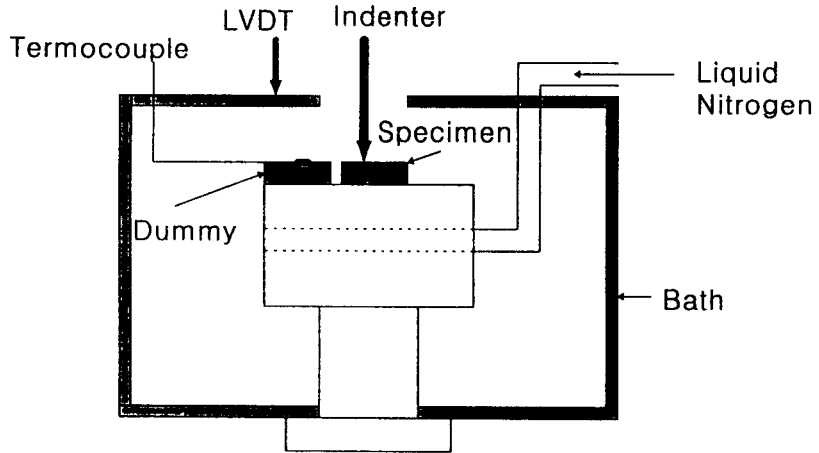


Fig. 1 Schematic of low-temperature ABI test set-up

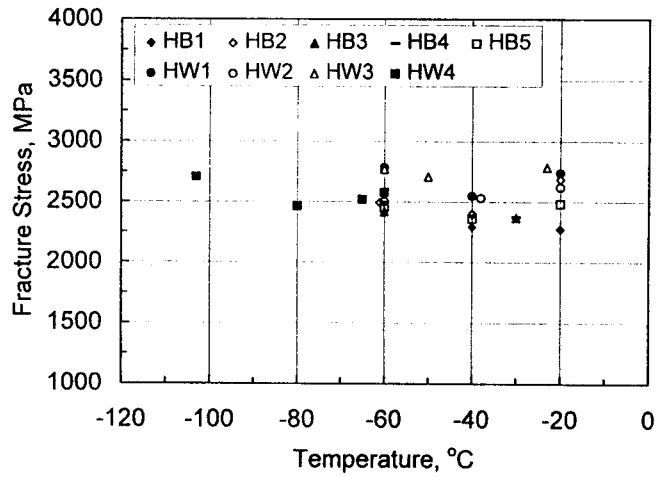


Fig. 2 Fracture stress(calculated) versus temperature

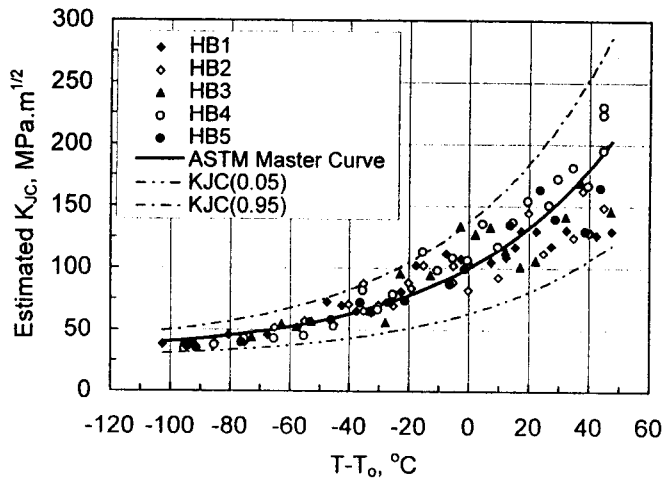


Fig. 3 Estimated K_{JC} of SA508 C1.3 steels (base metals)

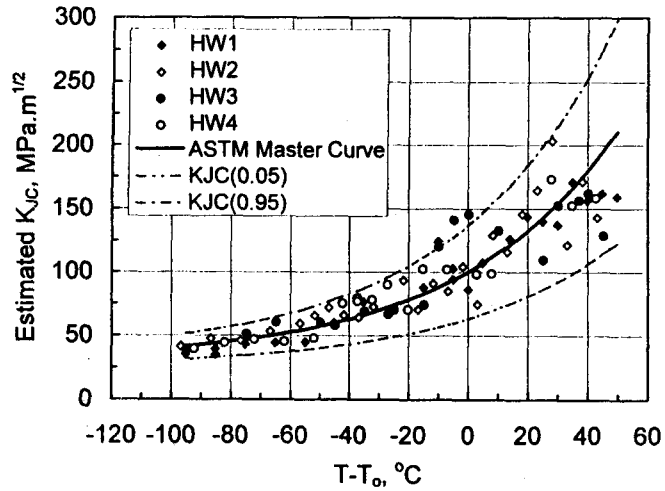


Fig. 4 Estimated K_{JC} of RPV weld metals

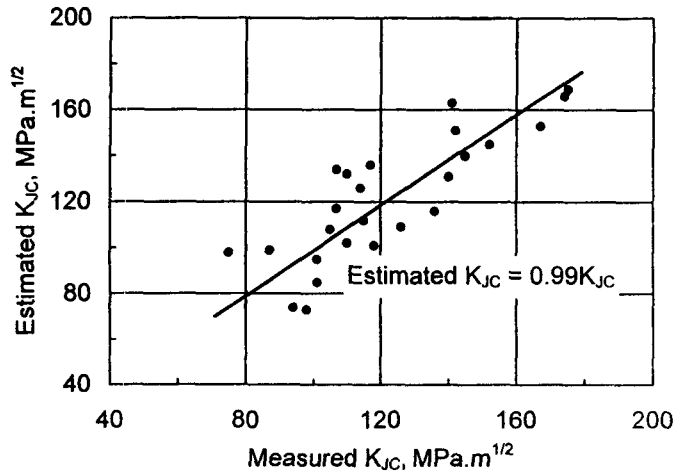


Fig. 5 Comparison of estimated K_{JC} with measured K_{JC}

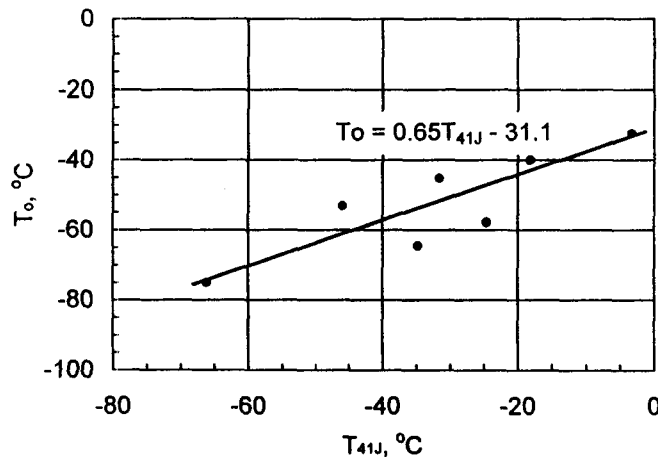


Fig. 6 Correlation between the reference temperature, T_0 , and the index temperature of Charpy impact energy, T_{41J}